

# On rotations in front-form dynamics

Uwe Trittmann<sup>a</sup> and Hans-Christian Pauli<sup>b</sup>

<sup>a</sup>*Department of Physics, Ohio State University, Columbus, OH, USA*

<sup>b</sup>*Max-Planck-Institut für Kernphysik, Heidelberg, Germany*

---

## Abstract

Quantum field theories in front-form dynamics are not manifestly rotationally invariant. We study a model bound-state equation in 3+1 dimensional front-form dynamics, which was shown earlier to reproduce the Bohr and hyperfine structure of positronium. We test this model with regard to its rotational symmetry and find that rotational invariance is preserved to a high degree. Also, we find and quantify the expected dependence on the cut-off.

---

The framework of Discretized Light Cone Quantization (DLCQ) has been applied successfully to many and diverse physical systems, *cf.* Ref. [1] and references therein. The method is especially efficient when applied in lower dimensions, and seems ideally suited for strictly two-dimensional systems [2,3]. The extension of the DLCQ program into the physical four dimensions is both necessary and exciting, even when some of its striking advantages are lost on the way. Several attempts to do so were hampered by a prominent draw-back of the front form, particularly its lack of manifest rotational symmetry; but recently some progress has been made [4].

The method of DLCQ was applied to 3+1 dimensions first by Tang *et al.* [5], to check the method at the example of positronium. This approach, like others [6] trying to solve the matrix eigenvalue problem by using a light-cone adapted Tamm-Dancoff procedure, suffered severe convergence problems. Wilson and collaborators [7] considered the problem in more abstract terms, emphasizing the role of renormalization problems. But one may state in all fairness that concrete and practical prescriptions have not emanated thus far. Their positronium spectrum [8] was obtained later. Within the model of Krautgärtner, Pauli and Wölz [9], however, the Bohr and the hyperfine structure of positronium on the light-front was resolved, but only for the z-component of total angular momentum  $J_z = 0$ . The derivation of the effective interaction was not overwhelmingly convincing, and the problems with a cutoff-dependent eigenvalue equation have not been settled thus far, see however also Ref. [10].

But even with the apparent shortcomings of this model, one can examine its rotational symmetry by asking whether the corresponding members of a rotational multiplet are degenerate or not, and if the multiplets contain the correct number of degenerate states. The agenda is then quite obvious:

- Generalize the method to arbitrary  $J_z$ ;
- Increase the numerical accuracy needed for that.

If we can calculate the eigenvalue spectrum separately for each  $J_z$ , which is a kinematic operator both in the front and in the instant form [11], some of the eigenvalues of distinct  $J_z$  must be degenerate and form a multiplet, also in the front form. We can thus investigate *quantitatively* to which extent rotational symmetry is violated within a specific model. Any violation of the degeneracy of multiplets is a strong indication that the original covariance of the Lagrangian was lost by nature of the (model dependent) approximations.

## 1 Model positronium

The model of positronium considered here has been introduced by Krautgärtner *et al.* [9] and we refer to it for all unquoted details. In light-cone quantization, the contraction of the momentum operators  $P^\mu$ , is called the light-cone Hamiltonian,  $H_{\text{LC}} = P^\mu P_\mu$ . Solving the eigenvalue problem

$$H_{\text{LC}}|\Psi\rangle = M^2|\Psi\rangle, \quad (1)$$

yields the mass (squared) eigenvalue spectrum of a physical system. This full problem is very difficult to solve, particularly in gauge theory, see [12]. It is easier to solve the problem in a reduced space with an effective Hamiltonian [13]

$$H_{\text{LC}}^{\text{eff}}|\psi\rangle = (T + U^{\text{eff}})|\psi\rangle = M^2|\psi\rangle, \quad (2)$$

with some free kinetic part  $T$  and an effective interaction  $U^{\text{eff}}$ . The reduced space is here the Fock space of the single electron and a single positron, *i.e.*  $|\psi\rangle \equiv |\Psi_{e\bar{e}}\rangle$ . In what follows, we denote the mass, the longitudinal momentum fraction, the transverse momentum, and the helicity of the electron with  $m, x, \vec{k}_\perp$ , and  $\lambda_e$ , respectively, and those of the positron with  $m, 1 - x, -\vec{k}_\perp$ , and  $\lambda_{\bar{e}}$ . Physically, the effective interaction scatters an electron-positron pair from a state with four-momenta  $(k_e, k_{\bar{e}})$  into a state with  $(k'_e, k'_{\bar{e}})$ , which in general has a different free invariant mass than the entrance channel. This requires a certain amount of symmetrization which was made in all previous

work [14,15], and thus also in [9]. A more thorough discussion can be found Ref. [17]. This in mind, Eq. (2) becomes an integral equation

$$M_n^2(x, \vec{k}_\perp; \lambda_e, \lambda_{\bar{e}}|\psi_n) = \frac{m^2 + \vec{k}_\perp^2}{x(1-x)} \langle x, \vec{k}_\perp; \lambda_e, \lambda_{\bar{e}}|\psi_n \rangle \quad (3)$$

$$- \frac{\alpha}{2\pi^2} \sum_{\lambda'_e, \lambda'_{\bar{e}} \in D} \int \frac{dx' d^2\vec{k}'_\perp}{Q^2} \langle x, \vec{k}_\perp; \lambda_e, \lambda_{\bar{e}}|S|x', \vec{k}'_\perp; \lambda'_e, \lambda'_{\bar{e}} \rangle \langle x', \vec{k}'_\perp; \lambda'_e, \lambda'_{\bar{e}}|\psi_n \rangle.$$

Symmetrization is reflected in the denominator

$$Q^2(x, \vec{k}_\perp; x', \vec{k}'_\perp) = -\frac{1}{2} [(k_e - k'_e)^2 + (k_{\bar{e}} - k'_{\bar{e}})^2], \quad (4)$$

which is the mean Feynman four-momentum transfer. The Lorentz-contracted Dirac spinors are collected in

$$\langle \lambda_e, \lambda_{\bar{e}}|S|\lambda'_e, \lambda'_{\bar{e}} \rangle = [\bar{u}(k_e, \lambda_e)\gamma^\mu u(k'_e, \lambda'_e)] [\bar{v}(k'_{\bar{e}}, \lambda'_{\bar{e}})\gamma_\mu v(k_{\bar{e}}, \lambda_{\bar{e}})]. \quad (5)$$

In helicity space it is a  $4 \times 4$  matrix which is tabulated explicitly in the Compendium [16] or in Ref. [18, App. B]. The domain of integration  $D$  is specified by the ‘sharp’ cut-off  $\Lambda$

$$m^2 + \vec{k}'_\perp{}^2 \leq x'(1-x')(\Lambda^2 + 4m^2), \quad (6)$$

*i.e.* by Lepage-Brodsky regularization [15]. The experimental literature differentiates between proper positronium ( $\mu\bar{e}$ ) and true positronium ( $e\bar{e}$ ) (Telegdi). The model in Eq.(3) is neither of the two: It is ‘model positronium’. The annihilation channel is however included in Refs. [17–19].

In the meantime, the inherent difficulties with the light-cone adapted Tamm-Dancoff approach have faded away, since better formalisms yield the very same integral equation (3), see *f.e.* [10]. Note that the above equation is actually a set of four coupled integral equations in the three variables  $x$ ,  $k_x = |\vec{k}_\perp| \sin \varphi$  and  $k_y = |\vec{k}_\perp| \cos \varphi$ . Its numerical solution is highly non-trivial.

## 2 The construction of the multiplets and the numerical results

From usual (instant form) quantization one is used to the fact that the Hamiltonian commutes with the total angular momentum operator  $\mathbf{J}^2$  with eigenvalues  $J(J+1)$ . As a consequence, the Hamiltonian eigenvalues are  $(2J+1)$ -fold

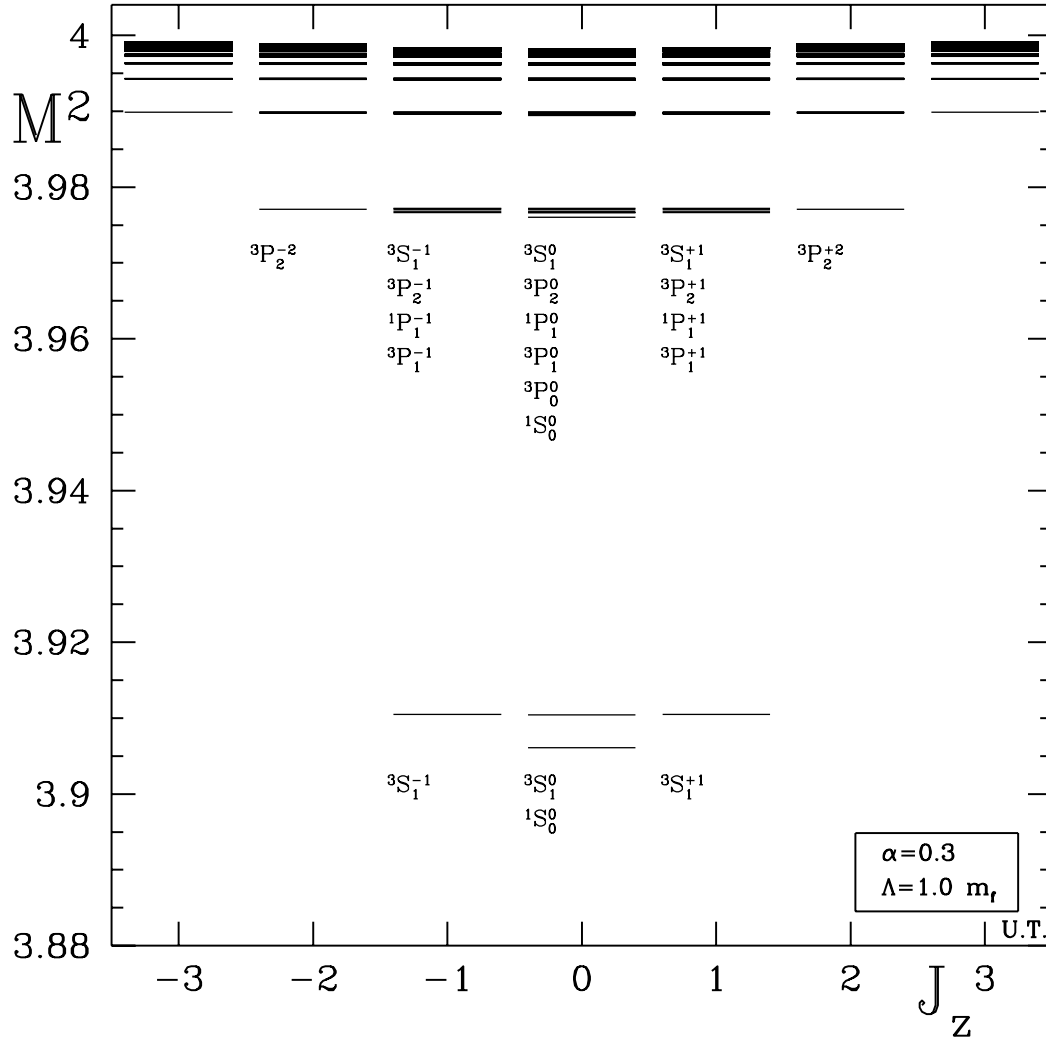


Fig. 1. The spectrum of the positronium model for  $|J_z| \leq 3$  at  $\Lambda = m$ ,  $N_1 = N_2 = 21$ . The eigenvalues  $M$  are given in units of the electron mass  $m$ . – The multiplet structure of the eigenvalues is emphasized by the phenomenological notation  $^{2S+1}L_J^{J_z}$ .

degenerate. The individual members of a  $\mathbf{J}^2$ -multiplet are labeled by  $J_z$ . In the front form things are different:  $J_z$  is the only kinematic of the three rotation operators. The key observation here is that front-form eigenstates can be classified by  $J_z$  but not by a quantum number with respect to  $\mathbf{J}^2$ . We can, however, diagonalize the Hamiltonian subsequently in different sectors characterized by  $J_z$ , *i.e.* as a function of  $J_z = 0, \pm 1, \pm 2, \dots$ . Some of the eigenvalues will be degenerate in  $J_z$ , within a certain numerical accuracy of course, and form the usual (instant form) multiplets. The largest value of  $J_z$  in a given multiplet determines the multiplicity,  $2(J_z)_{\max} + 1$ , and thus indirectly the quantum number  $J$ . If we find these degenerate multiplets, we have reproduced the multiplet structure of the instant form. The question is then to which extent multiplets are degenerate, *i.e.* on which level of accuracy rotational invariance is violated.

Our prejudices are illustrated in Fig. 1. Here is our most important result, and we shall explain below how to get it. The figure has the anticipated properties: the eigenvalues are arranged in degenerate multiplets, and each multiplet has an odd number of members. The eigenvalues can be arranged in clusters which are characterized by the Bohr quantum number  $n$ . For a pure Coulomb spectrum there would be  $(4n - 2)$  degenerate states with spin projection  $J_z = 0$ , and we found that the multiplets in our calculations pass this check: they have precisely  $(4n - 2)$  members. We have observed this property up to  $n=5$ , beyond which we have seen no reason to pursue.

Another important result is that only those combinations of the quantum numbers  $\pi_{\mathcal{C}}$  and  $\pi_{\mathcal{H}}$  appear which are expected from a non-relativistic analysis. Usually one classifies the states with the spectroscopic notation  $^{2S+1}L_J$ . In front-form dynamics, however, neither the total angular momentum  $J$ , nor the orbital angular momentum  $L$ , nor the total spin  $S$  are good (kinematic) quantum numbers. Rather, the front-form Hamiltonian is symmetric under charge conjugation  $\mathcal{C}$  and a combination of time reversal  $\mathcal{T}$  and parity  $\mathcal{P}$ , sometimes called *handedness*  $\mathcal{H} \equiv \mathcal{P}\mathcal{T}$ . In the non-relativistic case, one can relate the (instant form) quantum numbers  $(J, L, S)$  uniquely to the (front form) quantum numbers  $(\pi_{\mathcal{C}}, \pi_{\mathcal{H}})$ , if one chooses a certain convention for the time reversal operation [20]. The spectroscopic notation is used only to label the states conveniently [17–19].

The multiplets of mass (squared) eigenvalues are seemingly degenerate on the scale of the figure (Fig. 1). To be more quantitative we collect in Table 1 the first 18 eigenvalues in the form of binding coefficient defined by

$$B_n(J_z) = \frac{4}{m\alpha^2} (2m - M_n), \quad (7)$$

where the trivial dependence on mass and coupling constant is removed. The numerical errors (in parenthesis) are estimated from the difference between the values for maximal and next to maximal number of integration points. Except for a few states to be discussed below, the relative discrepancy of corresponding eigenvalues is typically a few parts in  $10^5$ , *i.e.* the degeneracy is on the level of numerical errors of the diagonalization routine.

The positronium spectrum has been calculated perturbatively, long ago by [21] and [22], and we have to keep in mind that these calculations were done under the *proviso* of the small  $\alpha \sim 1/137$ . Despite that, our eigenvalues agree quite well, *i.e.* on the percent level, with those results, even for the highly excited states, see Table 1.

The singlets  $^1S_0$  tend to be too weakly bound, especially for the low Bohr quantum numbers  $n = 1$  and  $n = 2$ . This effect is reversed for the triplets  $^3S_1$ .

Table 1

The binding coefficients  $B_n$  for  $\alpha = 0.3$ ,  $\Lambda = m$ ,  $N_1 = N_2 = 21$ . — Column 1 gives the spectroscopic notation  $n^{2S+1}L_J$  and column 2 the parities  $\mathcal{C}$  and  $\mathcal{H}$ . The numerical errors of  $B_n$  (in parenthesis) are estimated, see text. The last column lists the discrepancy to perturbation theory up to order  $\mathcal{O}(\alpha^4)$  [22].

| Term      | $\pi_{\mathcal{C}}\pi_{\mathcal{H}}$ | $B_n(0)$    | $B_n(1)$    | $(B_n(0) - B_n(1))$ | $\Delta B_n(\text{pert})$ |
|-----------|--------------------------------------|-------------|-------------|---------------------|---------------------------|
|           |                                      |             |             | $\times 10^5$       | in %                      |
| 1 $^1S_0$ | + -                                  | 1.04955(2)  |             |                     | -6.13                     |
| 1 $^3S_1$ | - +                                  | 1.00101(11) | 1.00038(7)  | 63.5                | -0.29                     |
| 2 $^1S_0$ | + -                                  | 0.26024(17) |             |                     | 3.13                      |
| 2 $^3S_1$ | - +                                  | 0.25380(22) | 0.25372(21) | 8.33                | -0.07                     |
| 2 $^1P_1$ | - -                                  | 0.25797(16) | 0.25798(17) | -1.30               | -1.71                     |
| 2 $^3P_0$ | + +                                  | 0.26707(16) |             |                     | -2.27                     |
| 2 $^3P_1$ | + -                                  | 0.25967(21) | 0.26008(16) | -40.8               | -1.63                     |
| 2 $^3P_2$ | + +                                  | 0.25526(18) | 0.25525(17) | 0.47                | -1.69                     |
| 3 $^1S_0$ | + -                                  | 0.11521(31) |             |                     | 1.54                      |
| 3 $^3S_1$ | - +                                  | 0.11344(36) | 0.11341(26) | 2.79                | -0.77                     |
| 3 $^1P_1$ | - -                                  | 0.11449(27) | 0.11453(28) | -3.96               | -1.71                     |
| 3 $^3P_0$ | + +                                  | 0.11713(27) |             |                     | -2.04                     |
| 3 $^3P_1$ | + -                                  | 0.11513(33) | 0.11512(27) | 1.13                | -1.77                     |
| 3 $^3P_2$ | + +                                  | 0.11372(28) | 0.11372(28) | -0.26               | -1.72                     |
| 3 $^1D_2$ | + -                                  | 0.11282(15) | 0.11284(16) | -2.66               | -1.02                     |
| 3 $^3D_1$ | - +                                  | 0.11343(16) | 0.11350(28) | -6.90               | -1.56                     |
| 3 $^3D_2$ | - -                                  | 0.11298(16) | 0.11298(16) | -0.43               | -1.06                     |
| 3 $^3D_3$ | - +                                  | 0.11251(16) | 0.11252(16) | -0.41               | -1.03                     |

Also, the ordering of the multiplets seems to have minor errors. For instance, the  $2^1S_0$  state and the  $2^1P_0$  state are permuted: the  $S$ -state should be the lowest according to perturbation theory. We convinced ourselves that this is a finite cut-off effect.

The numerical approach has two formal parameters: the number of integration points  $N_1 = N_2 = N$  and  $\Lambda$ . The dependence on the number of integration points  $N$  was found to decrease exponentially fast, even for the splitting between triplet states. The asymptotic value  $\Delta M^2(N \rightarrow \infty) = a$  amounts to only 0.5% of the relevant scale, namely the singlet-triplet splitting, of roughly  $0.0102m^2$ . With other words, the states are highly degenerate.

Table 2

The binding coefficients of the singlet ( $B_s$ ) and the triplet states ( $B_t$ ) for  $\alpha = 0.3$ ,  $N_1 = 25$ ,  $N_2 = 21$  are given as function of the cut-off  $\Lambda$ . They are compared with the results of perturbation theory [22] up to order  $\mathcal{O}(\alpha^4)$  and  $\mathcal{O}(\alpha^6 \ln \alpha)$ .

| cut-off $\frac{\Lambda}{m}$        | $B_s$      | $B_t$      | $C_{hf}$   |
|------------------------------------|------------|------------|------------|
| 1.0                                | 1.04903964 | 1.00046227 | 0.13493713 |
| 1.8                                | 1.16373904 | 1.06860934 | 0.26424917 |
| 3.6                                | 1.25570148 | 1.10111328 | 0.42941166 |
| 5.4                                | 1.29978050 | 1.11163578 | 0.52262422 |
| 7.2                                | 1.32941912 | 1.11782782 | 0.58775360 |
| 9.0                                | 1.35223982 | 1.12233652 | 0.63862028 |
| 10.8                               | 1.37112216 | 1.12596311 | 0.68099735 |
| 12.6                               | 1.38744792 | 1.12904455 | 0.71778713 |
| 14.4                               | 1.40198469 | 1.13175363 | 0.75064183 |
| 16.2                               | 1.41520247 | 1.13419048 | 0.78058886 |
| 18.0                               | 1.42740143 | 1.13641774 | 0.80828803 |
| $\mathcal{O}(\alpha^4)$            | 1.11812500 | 0.99812500 | 0.33333333 |
| $\mathcal{O}(\alpha^6 \ln \alpha)$ |            |            | 0.23792985 |

**The dependence on the cut-off  $\Lambda$ .** The weak point of the present work is the expected dependence on  $\Lambda$ . Its occurrence is not a particular feature of the light cone approach, but appears due to the Dirac interaction in any (gauge) field theory: For very large (transversal) momenta, *i.e.* for  $\vec{k}'^2 \gg \vec{k}_\perp^2$ , holds  $\langle \uparrow\downarrow |S| \uparrow\downarrow \rangle / Q^2 \rightarrow 2$  and  $\langle \downarrow\uparrow |S| \downarrow\uparrow \rangle / Q^2 \rightarrow 2$ : The kernel does not decay sufficiently fast, see also Ref. [10].

For discussing the dependence on  $\Lambda$  to some detail we present in Table 2 the binding coefficient for the singlet and the triplet together with the hyperfine coefficient

$$C_{hf} = \frac{1}{m\alpha^4} (M_{triplet} - M_{singlet}). \quad (8)$$

Its perturbative value [21,22] is known:

$$C_{hf} = \frac{1}{3} + \left[ \frac{1}{4} \right] - \frac{\alpha}{2\pi} \left( \ln 2 + \frac{16}{9} \right) + \mathcal{O}(\alpha^2 \ln \alpha). \quad (9)$$

The term in square brackets is the contribution from the one-photon annihilation. When comparing to previous results [9, Table V], we find that the

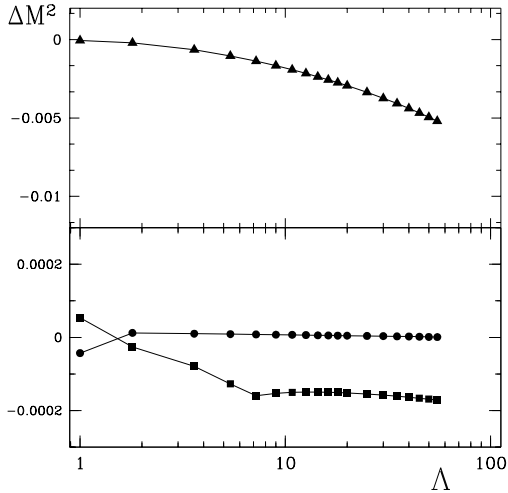


Fig. 2. The discrepancy function  $\Delta M_i^2$  ( $= M_i^2(1) - M_i^2(0)$ ), is plotted versus the cut-off  $\Lambda$  for the  $1^3S_1$  ( $\Delta$ ) [upper plot], the  $2^3P_1$ , and the  $2^1P_1$  ( $\bullet$ ) [lower plot]. Parameters are  $\Lambda = m$ ,  $N_1 = 21$ , and  $N_2 = 21$ .

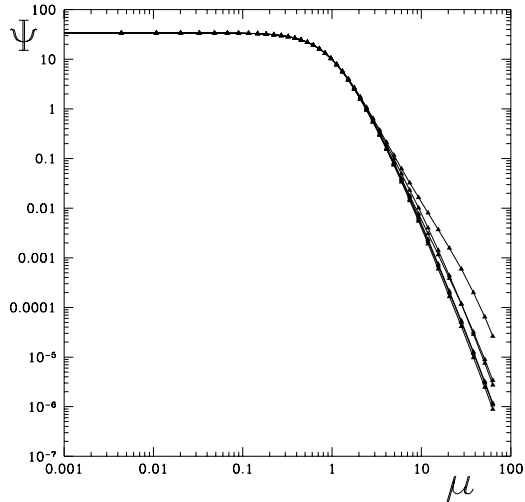


Fig. 3. The decrease of the  $J_z = 1$  triplet ground state wave function with parallel helicities as a function of the off-shell mass  $\mu$ . The parameters are  $\Lambda = 20.0 m$ ,  $N_1=41$ ,  $N_2=11$ . The six different curves correspond to six values of the angle  $\theta$ . Rotational symmetry is only for small  $\mu$ .

singlet falls off faster with  $\Lambda$ , yielding a smaller value for the hyperfine coefficient in our calculations. We note that the predictions of perturbation theory for different orders differ as much as 40% for the value of  $\alpha = 0.3$  used in the present work.

The degeneracy of eigenvalues as a function of the cut-off  $\Lambda$  is displayed in Fig. 2. One notices that the discrepancy between the triplet ground states rises from close to zero at  $\Lambda = m$  to roughly 50% of the hyperfine splitting for the large value of  $\Lambda = 50m$ . For the excited states the difference stays always below 12% on the relevant scale. Since we expect a logarithmic divergence we fit the curves  $M^2(\Lambda)$  to a polynomial in  $\ln \Lambda$ . If one omits the points for  $\Lambda > 20m$  because the integrations of the numerical counter term can become problematic in this region, the fit yields

$$\begin{aligned}
 M_{singlet}^2(\Lambda) &= \left( 3.90545 - 0.03510 \ln \frac{\Lambda}{m} + 0.00746 \ln^2 \frac{\Lambda}{m} \right) m^2, \\
 M_{triplet}^2(\Lambda) &= \left( 3.90976 - 0.01858 \ln \frac{\Lambda}{m} + 0.00789 \ln^2 \frac{\Lambda}{m} \right) m^2.
 \end{aligned} \tag{10}$$

The small coefficient of the  $\ln^2 \Lambda/m$ -term hints thus indeed at a logarithmic cut-off dependence of the eigenvalues. The dependence weakens if one includes the annihilation channel [19].



### 3 More details for general $J_z$ and the wavefunction

We want to calculate the Hamiltonian spectrum in all sectors of  $J_z$ . It is advantageous to reformulate the eigenvalue problem in such a way that allows for a separation of the sectors, *i.e.* a block diagonalization of the Hamiltonian with respect to the conserved quantum number  $J_z$ . By exploiting the symmetry of the Lagrangian under rotations in the  $(x, y)$  plane, we can substitute the angular variable  $\varphi$  by the quantum number  $J_z$  applying an integral transformation on Eq.(3), and in particular on the effective matrix elements

$$\begin{aligned} & \langle x, k_{\perp}, J_z; \lambda_e, \lambda_{\bar{e}} | \tilde{U}^{\text{eff}} | x', k'_{\perp}, J_z; \lambda'_e, \lambda'_{\bar{e}} \rangle \\ &= \frac{1}{2\pi} \int_0^{2\pi} \int_0^{2\pi} d\varphi d\varphi' e^{-i(L_z\varphi - L'_z\varphi')} \langle x, k_{\perp}, \varphi; \lambda_e, \lambda_{\bar{e}} | U^{\text{eff}} | x', k'_{\perp}, \varphi'; \lambda'_e, \lambda'_{\bar{e}} \rangle. \end{aligned} \quad (11)$$

It is easy to convince one-self that angular dependence can enter only in the form of the difference  $\varphi - \varphi'$ , and that the matrix elements are well-behaved for an arbitrary  $L_z = J_z - S_z$ . The eigenvalue problem, Eq. (3), looks now like

$$\begin{aligned} 0 &= \left( M_n^2 - \frac{m^2 + \vec{k}_{\perp}^2}{x(1-x)} \right) \langle x, k_{\perp}; \lambda_e, \lambda_{\bar{e}}; J_z | \psi_n \rangle \\ &+ \sum_{\lambda'_e, \lambda'_{\bar{e}}} \int dx' dk'_{\perp} \langle x, k_{\perp}; \lambda_e, \lambda_{\bar{e}} | \tilde{U}^{\text{eff}} | x', k'_{\perp}; \lambda'_e, \lambda'_{\bar{e}} \rangle \langle x', k'_{\perp}; \lambda'_e, \lambda'_{\bar{e}}; J_z | \psi_n \rangle. \end{aligned} \quad (12)$$

The angle averaged ‘general helicity table’  $\langle \lambda_e, \lambda_{\bar{e}} | \tilde{U}^{\text{eff}} | \lambda'_e, \lambda'_{\bar{e}} \rangle$  is again a  $4 \times 4$ -matrix in helicity space and tabulated in Refs. [17–19].

In the pioneering work of Krautgärtner *et al.* [9] Eq. (12) was solved numerically for the special case  $J_z = 0$ . By convenience they use momentum coordinates  $(\mu, \theta)$  instead of  $(x, k_{\perp})$ , corresponding to the Sawicki transformation in the Compendium [16]. The integral equation (3) is converted into a matrix equation by Gauss-Legendre quadratures in the off-shell mass  $\mu = 2|\vec{k}|$  and the polar angle  $\theta$ , with  $N_1$  and  $N_2$  integration points, respectively. The Hamiltonian matrix is subsequently diagonalized by numerical methods. In Ref. [9] the fine structure constant was set to the very large value  $\alpha = 0.3$  in order to resolve the accumulation of the eigenvalues around  $M^2 \simeq (2m)^2$ . We use the same unphysically large coupling to facilitate the search for possible violations of rotational symmetry in the spectrum. Because of the inherent quadratically integrable Coulomb singularity ( $Q^{-2}$ ) convergence of the eigenvalues with the number of the (Gaussian) integration points is extremely slow. Crucial improvement is achieved by using the Nyström method [23]. Its essence is to add a diagonal numerical (Coulomb) counter term and to subtract its discretized

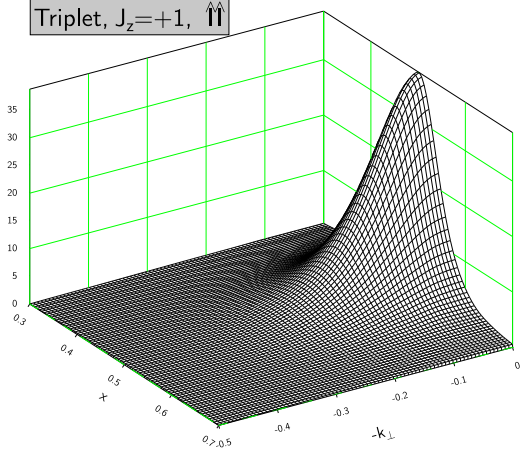


Fig. 4. Triplet wavefunction  $\psi_{\uparrow\uparrow}$  as a function of  $x$  and  $|\vec{k}_\perp|$ , at  $\varphi = 0$ .

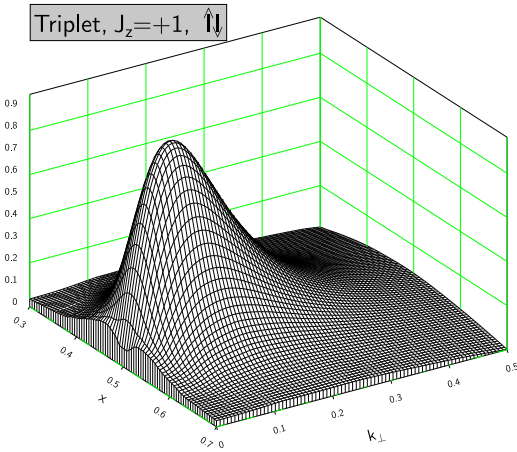


Fig. 5. Triplet wavefunction  $\psi_{\uparrow\downarrow}$  is for  $J_z = 1$ ,  $\Lambda = m$ ,  $N_1 = 41$ , and  $N_2 = 11$ .

version. In contrast to the pure Coulomb case, where the only counter term can be calculated analytically [24], the fine and hyperfine interactions in Eq.(3) require several counter terms. For  $J_z=0$  different diagonal matrix elements occur for parallel and anti-parallel helicities; they require two counter terms. Since both amplitudes have a similar singularity structure and comparable values, Krautgärtner *et al.* have used the same semi-analytical counter term in both diagonal matrix elements. Despite of this unnecessary simplification the convergence of the eigenvalues was satisfactory. In order to analyze the multiplet structure of the spectrum in all sectors of  $J_z$ , we have to improve the accuracy of this numerical algorithm. When  $J \neq 0$ , one has four different diagonal elements in the helicity matrix, one of which is much smaller than the others. To meet these numerical requirements, we avoid analytical treatment of the counter terms altogether, and integrate the counter terms numerically with a sufficiently high precision. This requires a somewhat larger computing time, but one is rewarded by an improvement of a factor two in convergence.

The wavefunctions are generated simultaneously with the spectrum. The two components of the lowest state ( $J_z = 0$ ) with anti-parallel and parallel helicities, look, up to a scaling factor, like the wavefunctions with parallel and anti-parallel helicities of Figs. 4-7, respectively. The shapes and the peak values are the same as in Ref. [9]. The plots in Ref. [9] seemed to indicate numerical problems because they showed internal structure. We found that this is due to numerical mistakes in the graphing package.

Let us discuss briefly the properties of the  $J_z=1$  wavefunctions, as displayed in Figs. 4-7. Due to the lower symmetry, the wave functions for  $J_z \neq 0$  show more structure than those for  $J_z = 0$ . The wave functions with  $J_z \neq 0$  have four components corresponding to the four different helicity combinations. We can see immediately from Figs. 5 and 6 that the components for anti-parallel helicities are identical. The components for parallel helicities in Figs. 4 and

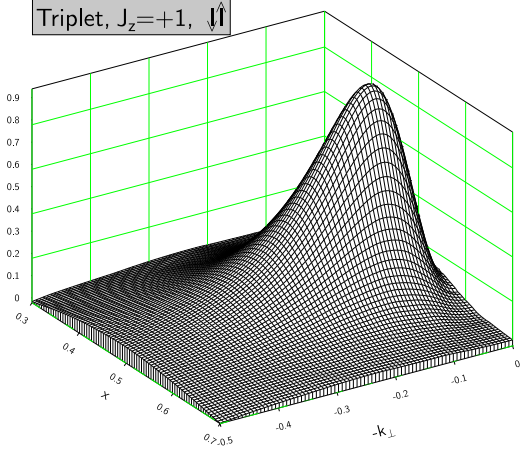


Fig. 6. Triplet wavefunction  $\psi_{\downarrow\uparrow}$ .

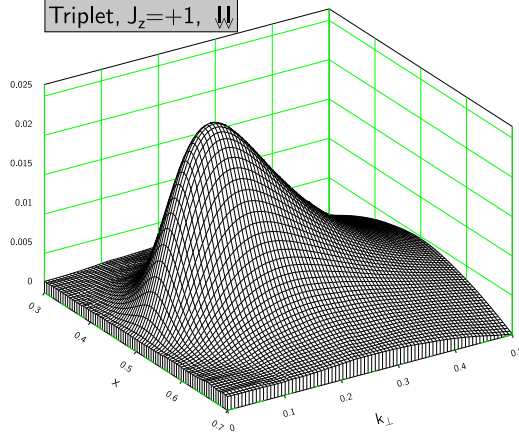


Fig. 7. Triplet wavefunction  $\psi_{\downarrow\downarrow}$ .

7 have rather disjunct properties: the  $(\uparrow\uparrow)$ -component peaks at  $x = 0.5$  and  $k_{\perp} = 0$  and is rotationally invariant. The  $(\downarrow\downarrow)$ -component vanishes at  $k_{\perp} = 0$  and is shaped more like the components with anti-parallel helicities. Note the very different peak values: the anti-parallel components are suppressed by a factor of 40 as compared to the  $(\uparrow\uparrow)$ -component, the  $(\downarrow\downarrow)$ -component is suppressed by a factor of 1400! We emphasize that the wave functions are *not* rotationally invariant, despite the fact that their non-relativistic analogue is an  $s$ -wave. One reason is the fact that rotations around the transverse axes are dynamical. Another way of seeing this is to transform the light-cone variables to quasi-equal-time coordinates. The Jacobian of the transformation breaks rotational invariance due to the term  $k_z^2/(m^2 + \vec{k}_{\perp}^2 + k_z^2)$ . The breaking of rotational invariance of the wave function is noticeable only for large momenta  $|\vec{k}| \gg m$ , or, correspondingly, large cut-offs  $\Lambda$ . As an example, the triplet wave function  $1^3S_1(\uparrow\uparrow)$  is plotted in Fig. 3 as a function of the off-shell mass  $\mu$ . Obviously, the wave function is not isotropic but depends on the angle  $\theta$  for sufficiently large values of the off-shell-mass. We note that with a cut-off of  $\Lambda = m$  in place, the discrepancy of curves with different  $\cos\theta$  would not be resolvable.

### Conclusions:

- (1) The counter term technology of Krautgärtner *et al.* [9] can be implemented without unnecessary simplifications.
- (2) The generalization to all values of the angular momentum projection  $J_z$  is possible and novel.
- (3) The dependence on the cut-off is logarithmic, and thus renormalizable.
- (4) Possible problems with rotational symmetry can be dealt with easier in practice than anticipated by more formal investigations in the literature.
- (5) The eigenvalues for different  $J_z$  arrange themselves in highly degenerate multiplets. This in turn lets us conclude that the effective interaction of Krautgärtner *et al.* [9] is consistent with the rotational thus Lorentz-invariance of the Lagrangian, and this holds probably for all light-cone based approaches.

## References

- [1] S.J. Brodsky, H.C. Pauli and S.S. Pinsky, Phys. Rep. **301** (1998) 299-486.
- [2] G.'t Hooft, Nucl. Phys. **B75** (1974) 461.
- [3] A. Bassetto and L. Griguolo, Phys. Lett. **B443** (1998) 325.
- [4] J. Carbonell, B. Desplanques, V.A. Karmanov and J.F. Mathiot, Phys. Rep. **300** (1998) 215-347.
- [5] A. Tang, S.J. Brodsky, and H.C. Pauli, Phys. Rev. **D44** (1991) 1842.
- [6] M. Kaluža and H.-C. Pauli, Phys. Rev. **D45** (1992) 2968-2981.
- [7] D. Mustaki, S. Pinsky, J. Shigemitsu, and K.G. Wilson, Phys. Rev. **D43** (1991) 3411; R.J. Perry, A. Harindranath, and K.G. Wilson, Phys. Rev. Lett. **65** (1990) 2959.
- [8] B.D. Jones, R.J. Perry, and S.D. Glazek, Phys. Rev. **D55** (1997) 6561-6583.
- [9] M. Krautgärtner, H.C. Pauli, and F. Wölz, Phys. Rev. **45** (1992) 3755-3774.
- [10] H.C. Pauli, this volume.
- [11] H. Leutwyler and J. Stern, Phys. Lett. **B69** (1977) 207.
- [12] J. Hiller, this volume.
- [13] P.M. Morse, H. Feshbach, Methods in Theoretical Physics, McGraw-Hill 1953.
- [14] I.J. Tamm, J. Phys. **9** (1945) 449; S.M. Dancoff, Phys. Rev. **78** (1950) 382.
- [15] G.P. Lepage and S.J. Brodsky, Phys. Rev. **D22** (1980) 2157.
- [16] Compendium, in the appendix to this volume.
- [17] U. Trittman, Ph.D. thesis, University of Heidelberg 1996; hep-th/9704215.
- [18] U. Trittman and H.C. Pauli, hep-th/9704215, hep-th/9705021.
- [19] U. Trittman, hep-th/9705072, hep-th/9706055.
- [20] K. Hornbostel, S.J. Brodsky, and H.C. Pauli, Phys. Rev. **D41** (1990) 3814.
- [21] E. Fermi, Z. Phys. **60** (1930) 320-333.
- [22] G.T. Bodwin, D.R. Yennie and C.J. Suchyta, Rev. Mod. Phys. **57** (1985) 723; S.N. Gupta, W.W. Repko and C.J. Suchyta, Phys. Rev. **D40** (1989) 4100-4104.
- [23] W. Hackbusch, Integralgleichungen, Teubner Verlag, Stuttgart 1989.
- [24] F. Wölz, master's thesis (diploma), University of Heidelberg 1990.